IOP PUBLISHING JOURNAL OF PHYSICS: CONDENSED MATTER

J. Phys.: Condens. Matter **21** (2009) 084210 (8pp) doi:10.1088/0953-8984/21/8/084210

Finding mechanism of transitions in complex systems: formation and migration of dislocation kinks in a silicon crystal

Andreas Pedersen[1], **Laurent Pizzagalli**[2] **and Hannes Jónsson**[1]

[1] Faculty of Science and Science Institute, University of Iceland, 107 Reykjavik, Iceland
[2] Laboratoire PHYMAT, CNRS UMR 6630, Université de Poitiers, BP 30179, 86962 Futuroscope Chasseneuil Cedex, France

Received 7 August 2008, in final form 18 November 2008
Published 30 January 2009
Online at stacks.iop.org/JPhysCM/21/084210

Abstract

We demonstrate how a saddle point search method can be used to study dislocation mobility in a covalent material—a non-trivial transition mechanism in a complex system. Repeated saddle point searches have been carried out by using the minimum mode following algorithm and dimer method in combination with several empirical potential functions for silicon in order to determine the mechanisms for the creation and migration of kinks on a non-dissociated screw dislocation in a silicon crystal. For the environment-dependent interatomic potential, three possible kink migration processes have been identified with activation energies of 0.17, 0.25, and 0.33 eV. The Lenosky potential gives a single, low energy migration mechanism with an activation energy of 0.07 eV, in good agreement with density functional theory results. The kink formation mechanism determined using this potential has an activation barrier of 1.2 eV. Calculations were also carried out with the Tersoff potential, Stillinger–Weber potential and Bolding–Andersen potential. The various potential functions give quite different results for the kink structure and the mechanism of transition.

(Some figures in this article are in colour only in the electronic version)

1. Introduction

An important task in computational materials science is the identification of thermally activated transitions that can occur in materials. Characterization of such transitions involves identifying the mechanism on the atomic scale and estimation of the transition rate. At first sight, it might seem that numerical simulations of the classical dynamics of the atoms, i.e. finite difference solution of Newton's equation of motion, would be a relatively straightforward way of reproducing laboratory experiments on materials and that one could simply observe the relevant processes from the dynamics simulations. Such classical dynamics calculations of atoms and molecules have, indeed, led to valuable insights and improved understanding of atomic scale processes in many diverse areas of science. However, direct classical dynamics simulations are limited to very short timescales, even when simple empirical potential functions are used to describe the atomic interactions—about a nanosecond of real time for a week of computations. This represents a severe limitation on the types of phenomena that can be studied in this way. Important processes such as diffusion and conformational changes are typically 'rare events', in that the atoms vibrate about their optimal position multiple times in between these events. For example, the activation energy for diffusion of a Si adatom on top of the Si(100) surface is about 0.6 eV [1]. Such a diffusion event occurs several times per second at room temperature and is active on the laboratory timescale. However, there are on the order of 10^{10} vibrational periods between diffusion events. A direct classical dynamics simulation, which has necessarily to faithfully track all these vibrational motions, would take on the order of a thousand years of computer time on present day computers before a trajectory corresponding to room temperature can be expected to show a single diffusion event! While the time between diffusion events can be decreased by raising the temperature, this does not provide a solution to the timescale problem because entropic effects can cause a crossover to a different mechanism at the higher temperature. It is clear that studies of thermally activated transitions cannot be carried out for typical systems by simply

simulating the classical dynamics of the atoms. It is essential to carry out the simulations on a much longer timescale [1] and use different algorithms. This timescale problem is one of the most important challenges in computational materials science.

The separation of timescales between vibrational motion and activated, configurational changes makes it possible to get accurate estimates of transition rates using purely statistical methods, namely transition state theory (TST) [2]. Apart from the Born–Oppenheimer approximation, TST relies on two basic assumptions: (a) the rate is slow enough that a Boltzmann distribution is established and maintained in the reactant state, and (b) a dividing surface of dimensionality $3N - 1$, where N is the number of atoms in the system, can be identified and the approximation is that a reacting trajectory going from the initial state to the final state only crosses the dividing surface once. The dividing surface must, therefore, represent a bottleneck for the transition. The TST expression for the rate constant can be written as

$$k = \frac{\langle |v| \rangle}{2} \frac{Q^{\ddagger}}{Q_R},$$

where $\langle |v| \rangle$ is the average speed along the normal, $Q^{\ddagger}$ is the configurational integral for the transition state dividing surface, and Q_R is the configurational integral for the initial state (the configuration integral for region S is $\int_S \mathrm{e}^{-V(\vec{R})/k_\mathrm{B}T}\,\mathrm{d}\vec{R}$ where $V(\vec{R})$ is the potential energy for configuration $\vec{R}$ of the atoms). The bottleneck can be of purely entropic origin, but for most activated transitions in materials it is due to an energy barrier between the two local minima on the energy surface representing initial and final states.

Since atoms in solids are usually tightly packed and the relevant temperature range is frequently low compared with the melting temperature, a harmonic approximation to the potential energy surface in the most important regions can typically be used in materials science studies without much loss of accuracy. This greatly simplifies the problem of estimating the rates. The transition state is then chosen to consist of hyperplanar segments going through saddle points on the potential energy ridge surrounding the initial state minimum and the normal of each segment is in the direction of negative curvature at the corresponding saddle point [3]. The rate constant for transition through each hyperplanar segment can be obtained from the energy and frequency of normal modes at the saddle point and the initial state [4]

$$k^{hTST} = \frac{\Pi_i^{3N} \nu_i^{\mathrm{init}}}{\Pi_i^{3N-1} \nu_i^{\ddagger}} \mathrm{e}^{-(E^{\ddagger} - E^{\mathrm{init}})/k_\mathrm{B}T}.$$

Here, $E^{\ddagger}$ is the energy of the saddle point, E^{init} is the local potential energy minimum corresponding to the initial state, and the ν_i are the corresponding normal mode frequencies. The symbol ‡ refers to the saddle point. The most challenging part in this calculation is the search for the relevant saddle points. Each saddle point represents a certain transition mechanism. The reaction coordinate at the saddle point is the direction of the unstable mode (the normal mode with negative eigenvalue). After a saddle point has been found, one can follow the saddle point along the unstable mode, both forward and backward, and map out the minimum energy path (MEP), thereby establishing what initial and final state this saddle point corresponds to. The identification of saddle points ends up being one of the most challenging tasks in studies of thermally activated transitions in materials.

When the initial and final state of a transition is known, an MEP connecting the two can be found relatively easily. A saddle point on the energy surface is then identified as a maximum along the MEP. In the nudged elastic band (NEB) method, a string of replicas of the system is generated using some interpolation between the initial and final state of the transition (usually a linear interpolation between the two end points, but also possibly including one or more intermediate configurations) [5, 6]. The replicas are connected with springs to control the distribution of images along the path and, thereby, the discretization of the path. If the same spring constant is used between all the replicas, the method results in an even spacing of the images along the MEP. Then, an optimization algorithm involving force projections is used to relax the replicas towards the MEP ('nudging'). With the 'climbing image' extension of NEB (CI-NEB), one of the images is made to converge on the highest saddle point along the MEP [5]. While the saddle point is the only important point for the harmonic TST rate estimate, in addition to the initial point, the MEP gives a useful, extended view of the potential energy landscape. For example, the optimal transition mechanism may involve a more complex path with one or more intermediate minima. This non-local view of the most relevant part of the potential energy landscape can be useful and ensures that the highest saddle point along the way—the rate limiting step—has been identified. It is important to remember that the NEB calculation converges on the MEP that is closest to the initial guess. Often, there is more than one MEP connecting a given initial and final state and the initial distribution of images chosen in the NEB calculation may lead to an MEP that has a higher activation energy than some other MEP. This feature of the method can be useful [7] but more often this represents a limitation of the method.

When multiple MEPs are present between given initial and final states, and when only the initial state of a transition is known, and both the final state and the mechanism of the transition are unknown, a search for the saddle points on the potential energy rim surrounding the initial state minimum can be conducted by climbing up the potential surface and converging on first order saddle points. This can be done using so called eigenvector following methods which are commonly used in studies of molecules and small clusters [8, 9]. Here, the Hessian matrix of second derivatives is constructed and then diagonalized to get the eigenvectors at each point along the climb. However, materials science simulations employing empirical potentials typically involve many atoms, on the order of a thousand, making eigenvector following unpractical because of the N^3 scaling. DFT calculations necessarily involve much smaller systems, on the order of 50–100, but ideally make use of plane waves as basis functions to eliminate boundary effects, and thereby cannot produce estimates of the second derivatives unless a great deal of computer time is involved. The minimum mode following method requires only

the first derivative of the energy and avoids having to solve the eigenvalue problem while maintaining the essential qualities of the eigenvector following method [10, 11]. By starting from an initial point that is obtained after random displacement from the initial state minimum and then following the lowest eigenmode from there (with no relaxation orthogonal to the lowest mode in the convex region), a distribution of saddle points can be obtained. Tests have shown that the lower energy saddle points tend to be found more often than less relevant, high energy saddle points [10]. Here, it is important to have a fast way of estimating the direction of the lowest mode without having to solve the full eigenvalue problem. One method to achieve this is the so called dimer method where two replicas of the system, a 'dimer', is constructed and is rotated about its center, with the separation distance fixed, in order to find the direction of the lowest frequency mode [10]. Then, the component of the force acting on the center of the dimer is reversed along the direction of the dimer. Any optimization algorithm which moves the dimer according to this modified force will then converge on a first order saddle point. The method has been illustrated by finding many possible diffusion mechanisms for an Al adatom on an Al(100) surface. In addition to the hop and two atom exchange processes, a four atom and three atom exchange process were also found, with almost equally low saddle points as the hop. At higher energy, a large number of processes were observed, some involving formation of a local reconstruction of the surface. In the present article, we illustrate the use of this method by a finding mechanism for the formation as well as migration of kinks on a dislocation in Si. After finding one or more saddle points and the corresponding final states, we find it useful to use the CI-NEB method, started with an interpolation through the saddle point configuration to map out the MEP.

We now turn to the application presented here. The plastic behavior of crystalline silicon in the ductile regime is known to depend on the mobility properties of 30° and 90° partial dislocations [12]. Both are assumed to move by formation of kink pairs and subsequent kink migration [13]. As a result, the structure of both the dislocation cores [14–19] and the kinks [20–24] have been widely investigated using atomistic numerical simulations. Despite these efforts, there is no consensus on the mechanism and activation energy for kink formation and kink migration in silicon. There are two reasons for this. First, a large number of kink configurations are possible for each partial dislocation [21], because of the dislocation core reconstructions and the possible role played by antiphase defects. Second, the simulation studies have mainly been carried out with empirical interaction potentials, but they are not reliable for describing strongly distorted structures such as dislocation kinks in covalent materials. Although the more precise density functional theory (DFT) calculations are feasible, the great number of configurations to be investigated and the large system size that is required make them difficult to perform. The mechanisms leading to kink formation and kink migration require determining saddle points on the high dimensional potential energy surface, and characterization of the full transition mechanism requires finding the minimum energy path. Since there are many kink configurations, one can expect a large number of possible MEPs leading to the creation and migration of dislocation kinks. The task is to determine the most favorable one, i.e. the one with the lowest activation energy. Since the NEB method converges only on the MEP that is closest to an initial guess, it is desirable to apply here a saddle point search method that samples the energy surface more widely. An NEB study starting from a 'reasonable' initial guess might miss a non-trivial mechanism giving the overall lowest activation energy. In principle, the minimum mode following method provides an unbiased search for all possible transition mechanisms that are feasible, if enough sampling is carried out.

In this article, we show how the minimum mode following method can be successfully used for investigating kink creation and migration in silicon. We focus on the screw dislocation, for which kink formation and migration has recently been studied with both empirical potential and DFT methods [25]. This system has the advantage of being relatively simple compared to silicon partial dislocations, and is thus well suited for examining the potential of the minimum mode following method in the case of extended defect mobility studies.

2. Methods

The simulated system is a piece of silicon crystal with a cubic diamond structure oriented along the $\hat{X} = [1\bar{2}1]$, $\hat{Y} = [111]$ and $\hat{Z} = [\bar{1}01]$ axis, including a non-dissociated screw dislocation aligned with $\hat{Z}$ and located in the middle of the system in the center of one hexagon [26]. There are 20 approximately square layers stacked along the $\hat{Z}$ axis and the total number of atoms is 16 800. Periodic boundary conditions are applied along the $\hat{Z}$ axis in order to model an infinite dislocation. To study the migration mechanism, two opposite kinks are introduced in the system, resulting in a kinked screw dislocation along the $\hat{X}$ direction (figure 1). The initial distance between the two kinks corresponds to 7 layers along $\hat{Z}$, which is large enough to make the kink–kink elastic interaction negligible. Finally, the system surfaces with $\hat{X}$ and $\hat{Y}$ as normals are free to relax in order to minimize surface effects.

Atomic interactions have been modeled using several empirical potentials: the environmental-dependent interaction potential (EDIP) [27], Lenosky [28], Tersoff [29], Stillinger–Weber [30] and Bolding–Andersen [31] potentials. For each of these, we have investigated the structure and stability of the kink configurations using a conjugate gradient minimization with a convergence criterion of 10^{-5} eV Å^{-1} in the maximal force.

The minimum mode following method [10] has been used to explore in an unbiased way the possible transition mechanisms. The idea behind the Dimer method is to locate saddle points on the potential energy surface (PES) near to the initial configuration. At the beginning of each saddle point search, the atoms within a radius of 4.0 Å from the atom in the center of a kink are displaced randomly. The norm of the displacement vector is scaled to 0.75 Å. When a saddle point

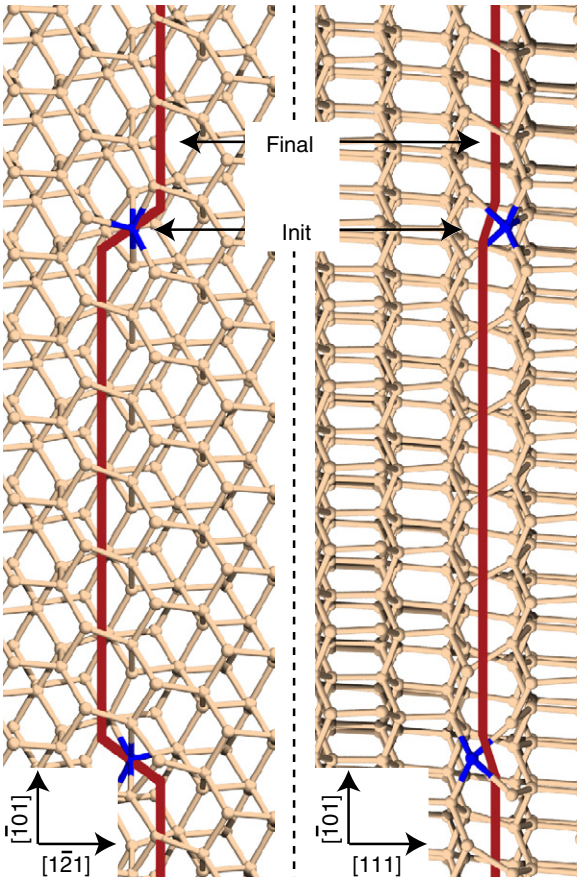

Figure 1. Structure of the initial configuration relaxed using EDIP potential. Left $\hat{X}\hat{Z}$-plane, right $\hat{Y}\hat{Z}$-plane. In the initial configuration the two kinks are separated by 7 atomic layers. The two processes of interest either separate the kinks further or bring them closer. The darker (blue) colored bonds connect to over-coordinated atoms—the kink-atoms in this configuration.

search is started, the initial estimation of the Hessian lowest eigenmode is done with 20 dimer rotational iterations, whereas only three rotational iterations are used when homing in on a saddle point. A search is considered to have converged when the total force vector has a norm below 25 meV Å^{-1}. For each system and interaction potential, a total of 200 saddle point searches were carried out starting to sample the saddle points on the energy surface.

The CI-NEB method has also been used to determine the full MEPs for the mechanisms revealed by the low energy saddle points. There, the band consisted of 28 replicas and the initial linear interpolation connected the initial and final configurations to the saddle point or an intermediate stable configuration, if the minimum mode following calculation had revealed its presence. The CI-NEB calculation was considered to have converged when the norm of the force vector for the image with the largest force was below 2.5 meV Å^{-1}. For calculations using the Tersoff potential a band of seven images is constructed by a linear interpolation directly connecting the relaxed endpoint configurations. For the latter mentioned calculation a less strict convergence criterion (50 meV Å^{-1}) was used.

3. Results

3.1. Kinks stability

The various empirical potential functions for Si give quite different results for the kink configuration. For the EDIP potential, the most stable kink configuration found is characterized by a central 5-coordinated atom, in agreement with previous calculations [25] (figure 1). We have considered a cut-off distance of 2.7 Å for defining bonds in the structural analysis. For the Lenosky potential, the lowest energy configuration includes a 3-coordinated atom in the center of the kink. This structure is similar to what is obtained from first-principles calculations [25]. The Tersoff potential gives a stable kink structure characterized by three 5-coordinated atoms. This configuration is similar to a metastable, intermediate transition structure obtained with the EDIP potential [25]. The Stillinger–Weber and the Bolding–Andersen potentials did not give a screw dislocation core located in the center of a hexagon. With these potentials, the most stable core is centered at a hexagon long bond. After kinks had been introduced in the system, relaxation led to spontaneous recombination and elimination of the kinks. As a consequence, we did not consider these two potential functions in studies of the transition mechanism using the minimum mode following and the CI-NEB methods.

3.2. Kink migration

When using the EDIP potential, we found many different possible transitions leading to an increase of the kink–kink separation distance along the $\hat{Z}$ axis. The three lowest energy saddle points found by the minimum mode following method give activation energies of 0.17, 0.26 and 0.33 eV and the corresponding prefactors have been determined to be 460, 490 and 820 GHz. The corresponding mechanisms, named M-I, M-II, and M-III in the following, have then been further analyzed in terms of structural changes by computing the MEPs with the CI-NEB method (figure 2). From the MEPs it is clear that for mechanisms M-I and M-III, the system passes through an intermediate stable configuration during the transition, whereas M-II is a direct transformation from the initial to the final configuration. The lowest energy mechanism M-I is the same as obtained from previous calculations [25], with an intermediate metastable configuration characterized by three 5-coordinated atoms. The migration mechanism is initiated by two atoms, labeled I1 and K2 in figure 3, moving toward each other, until the intermediate configuration is reached. In the second part of the transition, atoms I1 and K1 move again away from each other until the final configuration is obtained. In mechanism M-II, the saddle point configuration includes one 3-coordinated atom. Interestingly, this mechanism appears similar to what is obtained in first-principles calculations [25], although in the latter the transition energy is much lower. During the migration, atoms I1 and K2 (figure 3) move toward each other while I1 and K1 move away from each other until the final configuration is obtained. Finally, the third mechanism M-III, bears some similarities with M-II, with two quite similar saddle points. However, the M-III mechanism

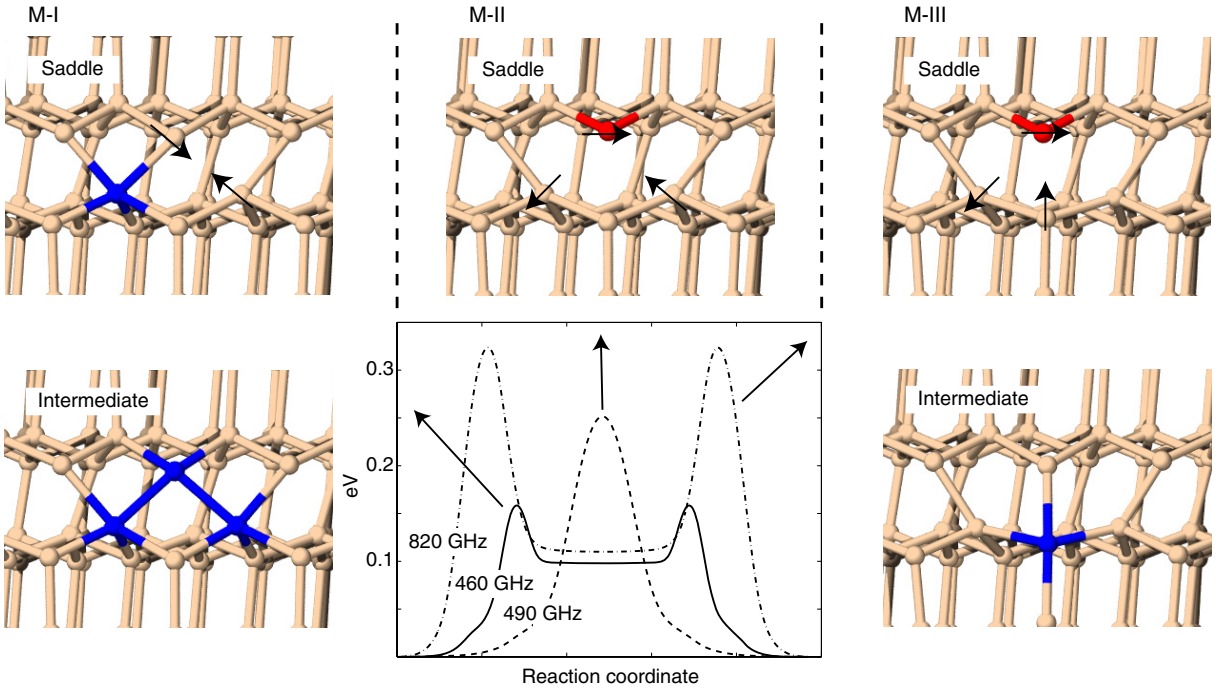

Figure 2. The three lowest energy migration mechanisms for a kink using the EDIP potential. The MEPs have been traced out with the CI-NEB method. Darker (blue) corresponds to five-fold coordination and brighter (red) corresponds to three-fold coordination. For M-I and M-III mechanisms an intermediate stable configuration is visited, whereas M-II is a direct transition from the initial to the final state. The saddle point configurations for M-II and M-III differ in that for M-II the three-fold coordinated atom is closer to the row below.

also involves an intermediate stable state, obtained by bonding the previously 3-coordinated atom (see figure 2). M-III is the most complex mechanism as I1 and K1 move away from each other while at the same time I1 and I2 move towards each other. These changes bring the system to the intermediate state. In the second part of the mechanism, I1 continuously moves towards K2 whereas I1 and I2 now move away from each other.

The searches performed using the Lenosky potential identified several saddle points, but only one of them connects the initial and final configurations of interest. This process has an activation energy of 0.07 eV. The mechanism is similar to M-II for the EDIP potential and no intermediate stable configuration occurs during the migration (lower mechanism in figure 4). The saddle point configuration where a bond has broken contains two extra 3-coordinated atoms. This preference for under-coordination by the Lenosky potential is consistent with the stable kink configuration containing a 3-coordinated atom while the stable configuration using EDIP contains a 5-coordinated atom.

For the Tersoff potential a migration barrier of 0.18 eV was determined by directly using the CI-NEB method. This mechanism involves an intermediate metastable structure characterized by one 5-coordinated atom while the initial, stable configuration includes three 5-coordinated atoms. The atomic displacements involved in the process are similar to those yielding the M-I mechanism found for the EDIP potential. The most stable configuration found for the Tersoff potential is similar to the intermediate structure obtained with the EDIP potential, and the intermediate configuration found for the Tersoff potential is the most stable structure found for the EDIP potential.

Table 1 summarizes the results for kink migration and compares the results obtained here using the empirical potentials with previous DFT calculations [25]. Although the empirical potentials give quite different outcomes, it is noteworthy that the lowest computed energy barrier is small in all cases, from 0.07 eV (Lenosky potential) to 0.18 eV (Tersoff potential). There is, then, an reasonably good overall agreement with DFT calculations, which gave an activation energy of 0.075 eV for a similar system. Among the empirical potentials, the Lenosky potential gives results that are most similar to DFT, in particular an almost equal energy barrier. It is also the only one of the empirical potentials that has a stable kink configurations with a central 3-coordinated atom, similar to the DFT calculations. Conversely, EDIP and the Tersoff potential tend to favor over-coordination rather than under-coordination, with one or several 5-coordinated atoms. Nevertheless, these two potentials might still be useful for modeling the mobility of screw dislocations by kink formation and migration. The estimated activation energy for these potentials is not that much larger than DFT results.

3.3. Kink pair creation

The mechanism for the creation of kinks was studied using the Lenosky potential, as this potential reproduced quite well the kink structure and migration results obtained by DFT calculations. To determine the kink pair creation mechanisms a series of 50 saddle point searches were carried out. Of the saddle points found, the creation of a kink pair is the fourth lowest and it involves a barrier of 1.19 eV and a

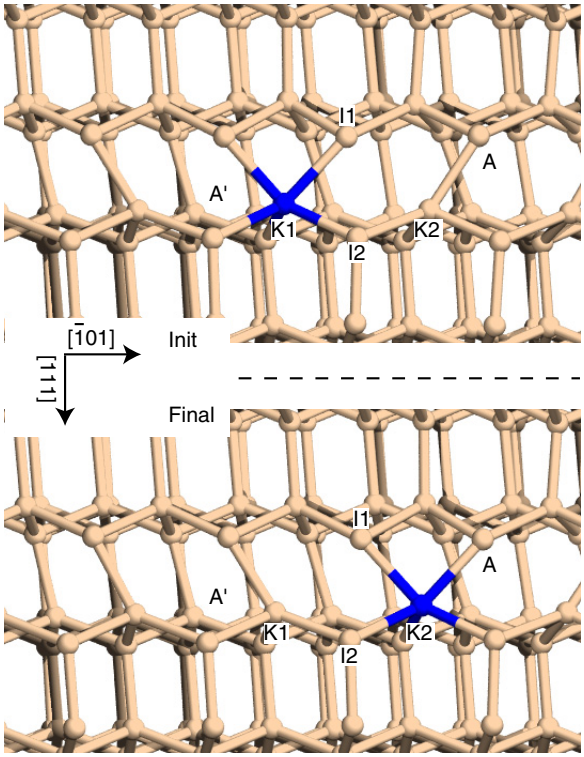

Figure 3. The initial and final configuration of the kink for the process where the kinks separate. In the initial configuration the kinks are separated by 7 atomic layers and in the final by 8 layers. A kink on a screw dislocation modeled with EDIP can be characterized by a five-fold coordinated atom (darker (blue) colored bonds), labeled K1 in the initial and K2 in the final configuration, all other atoms are four-fold coordinated. The two atoms labeled I1 and I2 are the atoms, besides K1 and K2, being displaced the most during the transitions from the initial to the final configuration.

Table 1. Calculated activation energy for kink migration using three different Si interatomic potentials compared with density functional theory results. The minimum energy path involves an intermediate stable state for two of the potentials.

	Barrier (eV)	Intermediate
Lenosky	0.07	No
EDIP	0.17	Yes
Tersoff	0.18	Yes
DFT	0.075 [25]	No

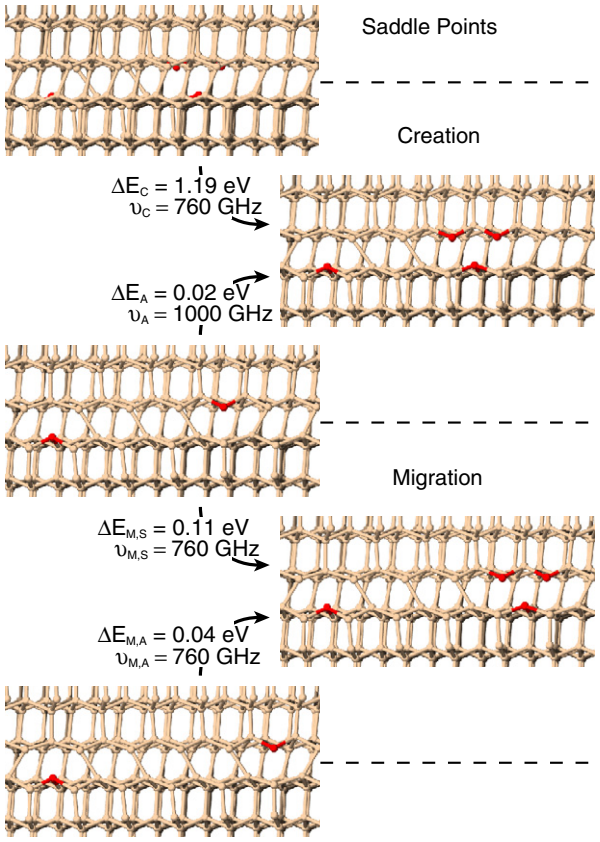

Figure 4. The creation and migration mechanism of kinks using the Lenosky potential. The color code is the same as in figure 2. The right column shows the saddle point configurations for creation (upper) and migration (lower). The upper is the creation mechanism involving a 1.19 eV barrier (ΔE_C) (the kinks have to be separated by 3 layers to obtain two stable kinks), whereas the barrier for annihilation of the kinks is only 0.02 eV (ΔE_A). Besides the difference in barrier energies there is also a slight difference in the prefactors, which for creation is 760 GHz (ν_C) and 1000 GHz for annihilation (ν_A). The lower shows the subsequent migration mechanism, the barrier for increasing separation ($\Delta E_{M,S}$) is initially larger than for decreasing separation ($\Delta E_{M,A}$) due to attractive kink–kink interaction (for non-interacting kinks the barrier is 0.07 eV). The prefactor for both migration mechanisms is 760 GHz ($\nu_{M,S}$ and $\nu_{M,A}$).

prefactor of 760 GHz (ΔE_C and ν_C in figure 4). The three lowest energy saddle points, which have energy of 0.90 eV and higher, correspond to the creation of a point defect. The kink pair configuration that is created is only weakly stable since annihilation and reconstruction of the perfect screw can occur with an energy barrier of only 0.02 eV and a prefactor of 1000 GHz (ΔE_A and ν_A). This attraction between the kinks is also manifested in the barrier for the first subsequent migration event, which is 0.11 eV ($\Delta E_{M,S}$), slightly higher than 0.07 eV as determined for the migration of non-interacting kinks. However, both migration mechanisms have a prefactor of 760 GHz ($\nu_{M,S}$ and $\nu_{M,A}$). The kink pair is created on the screw dislocation by passing through a saddle point configuration which contains three broken bonds. These three broken bonds result in four atoms being under-coordinated, consistent with the relatively high energy barrier. The structural rearrangement involves significant displacements of eight atoms that are in between the kinks, the central atoms moving the most.

4. Computational effort

The computational effort involved in finding the saddle points is best quantified by counting the total number of force and energy evaluations required for the minimum mode following calculations to reach convergence and the fraction of searches that lead to each of the low energy saddle points. This is summarized for the three lowest EDIP saddle points in table 2. Figure 5 shows the frequency with which the lowest 17 saddle points were found. The most important result is that the

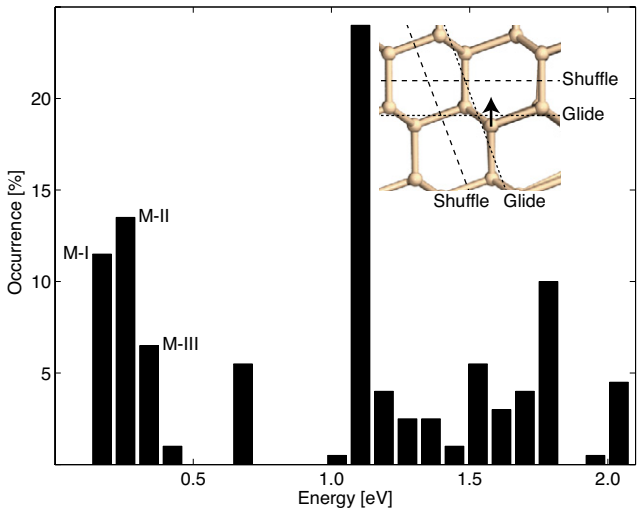

Figure 5. Relative occurrence of the 17 lowest saddle points found in 200 converged saddle point searches using the minimum mode following method and EDIP interaction potential. 31.5% of the searches lead to one of the three lowest energy saddle points. The inset shows the mechanism of the most frequently found saddle point which leads to the formation of a point defect.

Table 2. The computational effort, measured in the number of force/energy evaluations, for locating the three low energy migration mechanisms for the EDIP potential, based on 200 converged saddle point searches. FCs abbreviates forcecalls.

	Barrier (eV)	Times determined	Max FCs	Min FCs	Ave. FCs
M-I	0.17	23 [11.5%]	1725	252	713
M-II	0.26	27 [13.5%]	411	188	285
M-III	0.33	13 [6.5%]	506	146	231

three lowest energy saddle points, which are the important ones for migration, are among the five most frequently found saddle points. The M-III mechanism is determined less frequently than M-I and M-II, however. Other high energy mechanisms are shown in the figure 5, which correspond to transformations into configurations different from the final configurations of interest. It is important here to emphasize that the minimum mode following method locates saddle points without any bias, which means that all possible transitions whether or not they involve kink migration are potentially found. Statistics for the number of force/energy evaluations for the three lowest barrier mechanisms are reported in table 2. The lowest energy mechanism M-I requires the most force evaluations and is determined by 11.5% of the searches. For M-II and M-III, less force/energy evaluations are required in average. Note that the number of force/energy evaluations needed here is in accordance with the numbers given in [11] when taking into account the large number of degrees of freedom. In the case of the Lenosky potential, we found that the migration mechanism with the lowest barrier is the second most frequently determined mechanism, accounting for 16% of the searches. The average number of forcecalls was 976 in this case.

5. Summary

We demonstrated here how the minimum mode following method for finding saddle points can be used to do an extensive search for possible mechanisms leading to the formation and migration of kinks on a non-dissociated screw dislocation in silicon. This illustrates how the method can be used to identify the mechanism and determine the rate for non-trivial transitions in complex systems. For both the EDIP and the Lenosky potentials, we expect that we have obtained all possible lowest energy transitions for the kink migration. Three possible mechanisms have been identified for EDIP, with activation energies between 0.17 and 0.33 eV, whereas only one is obtained for the Lenosky potential with an activation energy 0.07 eV. The mechanism and the activation energy found using the latter potential is quite similar to the results obtained by DFT calculations [25]. We also considered the Tersoff potential, for which we found that the minimum energy kink migration occurs through yet another different process. Therefore, it appears that each potential yields a different mechanism.

Using the Lenosky potential, the kink pair creation mechanism has also been determined. To obtain the two stable kinks they need to be separated by at least three layers, which is why the creation process is a concerted displacement where as many as eight atoms are significantly displaced.

To conclude, the results presented here demonstrate how the minimum mode method can be used to investigate dislocation mobility and how much computational effort is involved. This method is powerful for easily exploring complicated high dimensional potential energy surfaces, as usually occurs for extended defects in covalent bonded materials. In fact, dislocation and kink structures for these materials generally involve complicated and non-intuitive bond reorganizations with many possible configurations. Using the minimum mode following method, we were able to determine several possible mechanisms for the kink migration and creation without any preconceived bias. Two point boundary methods, where both initial and final state need to be known a priori, such as the NEB and the CI-NEB methods result in a more limited sampling of possible mechanisms and involve a preconceived bias through the selection of the final state.

Acknowledgments

This work was supported by the Icelandic Research Fund (RANNIS), the Univ. of Iceland Research Fund, a Jules Verne travel award, and the 'Agence Nationale de la Recherche' (SIMDIM project No. ANR-06-BLAN-0250).

References

[1] Smith A P and Jónsson H 1996 *Phys. Rev. Lett.* **77** 1326
[2] Wigner E 1938 *Trans. Faraday Soc.* **34** 29
Eyring H 1935 *J. Chem. Phys.* **3** 107
[3] Jóhannesson G and Jónsson H 2001 *J. Chem. Phys.* **115** 9644
[4] Vineyard G H 1957 *J. Phys. Chem. Solids* **3** 121

[5] Henkelman G, Uberuaga B and Jónsson H 2000 *J. Chem. Phys.* **113** 9901
Jónsson H, Mills G and Jacobsen K W 1998 *Classical and Quantum Dynamics in Condensed Phase Simulations* ed B J Berne, G Ciccotti and D F Coker (Singapore: World Scientific) chapter 16, p 385
[6] Henkelman G and Jónsson H 2000 *J. Chem. Phys.* **113** 9978
[7] Pizzagalli L, Beauchamp P and Jónsson H 2008 *Phil. Mag.* **88** 91
[8] Cerjan C and Miller W 1981 *J. Chem. Phys.* **75** 2800
[9] Banerjee A, Adams N, Simons J and Shepard R 1985 *J. Phys. Chem.* **89** 52
[10] Henkelman G and Jónsson H 1999 *J. Chem. Phys.* **111** 7010
[11] Olsen R A, Kroes G J, Henkelman G, Arnaldsson A and Jónsson H 2004 *J. Chem. Phys.* **121** 9776
[12] Hirth J P and Lothe J 1982 *Theory of Dislocations* 2nd edn (New York: Wiley)
[13] Kolar H R, Spence J C H and Alexander H 1996 *Phys. Rev. Lett.* **77** 4031
[14] Duesbery M S, Joos B and Michel D J 1991 *Phys. Rev.* B **43** 5143
[15] Lehto N and Heggie M I 1999 *Properties of Crystalline Silicon* ed R Hull (London: INSPEC) p 357 (no. 20 in EMIS Datareviews)
[16] Bigger J R K, McInnes D A, Sutton A P, Payne M C, Stich I, King-Smith R D, Bird D M and Clarke L J 1992 *Phys. Rev. Lett.* **69** 2224
[17] Valladares A, White J A and Sutton A P 1998 *Phys. Rev. Lett.* **81** 4903
[18] Lehto N and Öberg S 1998 *Phys. Rev. Lett.* **80** 5568
[19] Miranda C R, Nunes R W and Antonelli A 2003 *Phys. Rev.* B **67** 235201
[20] Nunes R W and Vanderbilt D 2000 *J. Phys.: Condens. Matter* **12** 10021
[21] Bulatov V V, Yip S and Argon A S 1995 *Phil. Mag.* A **72** 453
[22] Bulatov V V, Justo J F, Cai W, Yip S, Argon A S, Lenosky T, de Koning M and de la Rubia T D 2001 *Phil. Mag.* A **81** 1257
[23] Huang Y M, Spence J C H and Sankey O F 1995 *Phys. Rev. Lett.* **74** 3392
[24] Öberg S, Sitch P K, Jones R and Heggie M I 1995 *Phys. Rev.* B **51** 13138
[25] Pizzagalli L, Pedersen A, Arnaldsson A, Jónsson H and Beauchamp P 2008 *Phys. Rev.* B **77** 064106
[26] Pizzagalli L, Beauchamp P and Rabier J 2003 *Phil. Mag.* A **83** 1191
[27] Justo J F, Bazant M Z, Kaxiras E, Bulatov V V and Yip S 1998 *Phys. Rev.* B **58** 2539
[28] Lenosky T J, Sadigh B, Alonso E, Bulatov V V, Diaz, Kim J, Voter A F and Kress J D 2000 *Modelling Simul. Mater. Sci. Eng.* **8** 825
[29] Tersoff J 1989 *Phys. Rev.* B **39** 5566
[30] Stillinger F H and Weber T A 1985 *Phys. Rev.* B **31** 5262
[31] Bolding B C and Andersen H C 1990 *Phys. Rev.* B **41** 10568